

# OPTIMIZATION STRATEGY FOR WIDE-BAND HARMONIC PROTECTION OF FLEXIBLE HVDC CONVERTER STATIONS CONSIDERING COMPLEX INRUSH CURRENTS OF CONVERTER TRANSFORMERS

Peng LI<sup>1</sup>, Haiwang JIN<sup>1</sup>, Mingxin GUO<sup>2</sup>, Wenbo YU<sup>1,3</sup>, Yibo ZHOU<sup>2,\*</sup>

*When a converter transformer with residual flux in its iron core undergoes energization, it may generate significant magnetizing inrush current while simultaneously inducing sympathetic inrush current in parallel-connected transformers due to magnetic coupling effects. The substantial harmonic components contained within these inrush currents can severely distort the busbar voltage waveform, resulting in temporary voltage depression and potentially triggering erroneous operations in wideband harmonic protection systems. To systematically address this critical issue, this paper conducts an in-depth investigation into the underlying physical mechanisms and system-wide impacts of complex inrush current phenomena in converter transformers, followed by a comprehensive analysis of wideband harmonic protection operational principles and key influencing factors affecting its performance during transient inrush conditions. An optimized wideband harmonic protection scheme based on a dynamic protection threshold is proposed. This method employs a real-time adaptive threshold that varies with the system operating state to mitigate protection maloperation caused by inrush current during operational transitions in HVDC transmission systems. A bipolar HVDC system simulation model is established to replicate the inrush current process during converter transformer energization, validating the effectiveness of the proposed method in practical engineering applications. Simulation results demonstrate that, compared to conventional fixed thresholds, the dynamic threshold-based protection algorithm significantly reduces the maloperation rate without introducing new failure scenarios, thereby enhancing the stability and reliability of the power system.*

**Keywords:** Inrush current of converter transformer; Broadband harmonic protection; Voltage distortion; Dynamic threshold

### Acronyms in this article

HVDC	High Voltage Direct Current	AC/DC	Alternating Current / Direct Current
CT	Current Transformer	MMC	Modular Multilevel Converter

### Symbols in all equations in this article

T1	No-Load Transformer	T2	operating transformer
----	---------------------	----	-----------------------

<sup>1</sup> State Grid Jibei Electric Power Co., Ltd. EHV Power Transmission Company, Beijing 102488, China;

<sup>2</sup> \* Key Laboratory of Modern Power System Simulation and Control & Renewable Energy Technology, Ministry of Education, Northeast Electric Power University, Jilin 132012, China, Corresponding author, Yibo Zhou, e-mail: mahunheioc8@163.com

<sup>3</sup> Hebei Key Laboratory of Equipment and Technology Demonstration of Flexible DC Transmission, Tianjin 300100, China.

$\Phi_1(0)/\Phi_2(0)$	initial core magnetic flux of T1/T2	$\Phi_1(t)/\Phi_2(t)$	Core Magnetic Flux of T1/T2
$R_{T1}/R_{T2}$	equivalent primary-side resistance of T1/T2	$L_{T1}/L_{T2}$	equivalent primary-side inductance of T1/T2
$I_{T1}/I_{T2}$	current through T1/T2	$I_s$	bus current
$L_s$	inductance of power source and bus	$X_{Ls}$	inductive reactance of voltage source and bus
$R_s$	resistance of power source and bus	$U_m$	amplitude of ac bus voltage
$\alpha$	switching angle	$\theta$	Impedance angle
$N_1$	number of primary winding turns	$K_{set}$	operating threshold of wide-frequency harmonic protection
$K$	operating coefficient of wide-frequency harmonic protection	$U_{rms}$	effective value of bus voltage full wave
$U_{1rms}$	effective value of fundamental component of bus voltage	$U_{rms}^h$	effective value of harmonic components of bus voltage
$U_c$	common point voltage	$f$	system operating frequency

## 1. Introduction

Against the backdrop of rapid growth in the renewable energy power generation sector and increasing demands for long-distance power transmission, high-voltage direct current (HVDC) transmission systems have garnered significant attention [1]. Converter transformer is one of the most important components in DC transmission system, which is responsible for providing power for converter, isolating AC and DC and suppressing short circuit current and various overvoltages. Compared with ordinary transformers, the working environment of the converter transformer is more severe, often facing a variety of high-frequency harmonic impact and interference in normal operation, the use of the earth as the inherent characteristics of the transmission circuit leads to the transformer is faced with the test of DC bias [2]. But the most important is the bipolar DC transmission system of various operating modes of change brought about by the impact of the above operations require the converter transformer frequently for the opening and closing operations [3]. A bipolar DC transmission system generally contains two or more transformers connected in parallel on the grid-side AC bus, in which a converter transformer may not only generate excitation inrush during the closing and charging process[4], but also trigger the converter transformer connected in parallel with it to generate sympathetic inrush[5] with small amplitude but slow decay, which may cause the inaccurate operation of the protection and result in various hazards. For example: generating a large number of harmonics to pollute the power grid, to the converter transformer and other equipment caused by thermal shock and

electromagnetic shock, triggering the protection, circuit breaker and so on the false operation, and so on [6-8]. All these are not conducive to the efficient and stable operation of the DC transmission system, so it is necessary to analyze the influence mechanism of converter transformers inrush current on the system protection from the principle and put forward the corresponding management strategy.

Literature [9] analyzes the impact of the excitation inrush of the converter transformer on the zero-sequence overcurrent protection of the line and puts forward the corresponding solution strategy for the problems found. Literature [10] analyzes the influence factors of excitation inrush, induction inrush and current transformer saturation, and for the problem of CT saturation caused by the DC component of converter transformers inrush, a new algorithm for CT saturation detection based on the second harmonic component is put forward to prevent this kind of misoperation, and literature [11] puts forward a new model for analyzing the over-saturation caused by the process of transformer switching and closing, while considering the impact of converter transformers inrush on the differential protection of line zero-sequence overcurrent, and puts forward corresponding solution strategies for the problems found. A new model is proposed to analyze the oversaturation phenomenon caused by the transformer switching process, while considering the effect of converter transformers inrush current on the differential protection. Literature [12] analyzes the influence of the residual magnetization intensity of an unloaded autotransformer on resonant overvoltage and proposes a set of effective measures to remove the residual magnetization of the autotransformer to suppress resonant overvoltage. Literature [13] focuses on the effect of the excitation inrush generated by the autotransformer on the differential protection, determines the optimal differential protection settings based on the simulation analysis, and calculates the probability of protection malfunction. Literature [14] for the transformer proposed based on the current and voltage ratio of the differential protection algorithm for simulation analysis and experimental verification, can prove the effectiveness of the differential protection for transformer inrush current and fault conditions. Owing to the unique characteristics of converter transformers and HVDC transmission systems, conventional protection strategies often prove inadequate in accurately and rapidly distinguishing between inrush currents and genuine fault conditions in differential protection schemes. To address this challenge, this study proposes an innovative approach focusing on the operating threshold of broadband harmonic protection. By implementing dynamic protection thresholds, the proposed method enhances protection reliability while ensuring the secure and efficient operation of HVDC transmission systems.

In this paper, starting from the impact of converter transformers inrush on the broadband harmonic protection, we analyze the converter transformer inrush mechanism and its influencing factors, the broadband harmonic protection

mechanism and action logic, and find out the key factors affecting the action coefficient of the broadband harmonic protection in the process of converter transformers inrush, and ultimately put forward a broadband harmonic protection optimization strategy with dynamically changing protection action thresholds according to the different operating states of the DC power transmission system. The optimization strategy of broadband harmonic protection is proposed according to the different operating states of DC transmission system.

Section 2 introduces the generation mechanism of inrush current in converter transformers, the magnetic flux formula, as well as the characteristics and hazards of inrush current. Section 3 elaborates on the operating logic of the wide-frequency harmonic protection algorithm, the calculation method for the operating coefficient, and analyzes the impact of converter transformer inrush current on the protection operating coefficient. Section 4 discusses the necessity of dynamic protection operating thresholds and proposes methods to address the influence of different factors on the protection operating coefficient. Subsequently, the article explains how to apply dynamic protection operating thresholds in practical engineering.

Section 5 establishes a simulation model of parallel inrush current in converter transformers, visually demonstrating the influence of the aforementioned factors on protection operation and introducing the calculation method for dynamic protection operating thresholds. Additionally, it compares the reliability of static and dynamic protection operating thresholds in responding to different fault types. The final section summarizes the proposed method and its simulation verification results, while also outlining potential future research directions.

## 2. Mechanism and impact of inrush current in converter transformers

### 2.1 Mechanism of Inrush Current in Converter transformers

The HVDC transmission system is composed of AC bus, converter transformers and converter. Taking MMC HVDC transmission system as an example, the grid side part can be simplified as in Fig. 1.

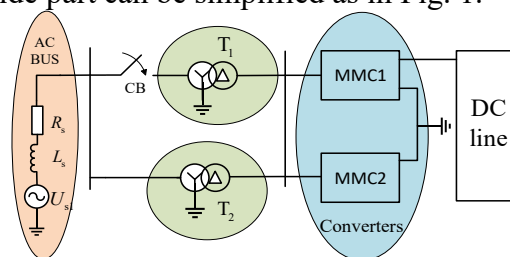


Fig. 1 MMC HVDC topology map

In a bipolar HVDC transmission system, the positive and negative converter transformers are connected in parallel. If the no-load converter transformer  $T_1$  is closed, it will generate inrush current. Affected by  $T_1$ , the converter transformer  $T_2$

normally operating will produce parallel sympathetic inrush. In order to simplify the calculation and facilitate analysis, the operating converter transformer is also considered as no-load. At the same time, the above model is simplified to obtain the simplified model shown in Fig. 2

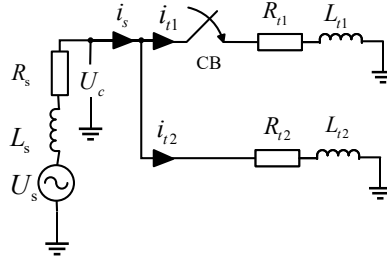


Fig. 1 Simplified equivalent circuit for inrush current in parallel converter transformers

Transformers operating in parallel generally have the same parameters, which can be identified as  $R_{t1} = R_{t2} = R$ ,  $L_{t1} = L_{t2} = L$ , and accordingly the magnetic chain expressions for the two converter transformers can be obtained as follows, respectively:

$$\Phi_1(t) = \frac{L_s + L}{ZN_1} U_m \sin(\omega t + \alpha - \theta) - \frac{1}{2} [\Phi_1(0) - \Phi_2(0)] e^{-\frac{R+2R_s}{L+2L_s} t} + \frac{1}{2} [\Phi_1(0) - \Phi_2(0)] e^{-\frac{R}{L} t} \quad (1)$$

$$\Phi_2(t) = \frac{L_s + L}{ZN_1} U_m \sin(\omega t + \alpha - \theta) - \frac{1}{2} [\Phi_1(0) - \Phi_2(0)] e^{-\frac{R+2R_s}{L+2L_s} t} - \frac{1}{2} [\Phi_1(0) - \Phi_2(0)] e^{-\frac{R}{L} t} \quad (2)$$

In the formula  $Z = \sqrt{(R + 2R_s)^2 + (L + 2L_s)^2}$ ,  $\theta = \arctan \frac{L+2L_s}{R+2R_s}$ ,  $\Phi_1(0)$ ,  $\Phi_2(0)$  are the core fluxes of T1 and T2 at the moment of no-load closing of the converter transformer, where  $\Phi_1(0)$  can be regarded as the initial remanent magnetization of the converter transformer T1. The above formula can be seen, the closing moment of the converter transformer still maintains the original magnetic flux unchanged, but after half a cycle of idle converter transformer magnetic flux reached its maximum value and then gradually decay, with its operation of the converter transformer internal flux and the closing of the converter transformer flux in the opposite direction, the amplitude is the first increase and then decrease after a long time to decay to the normal level.

## 2.2 Analysis of the impact of converter transformer inrush current

Due to the electromagnetic saturation characteristics of ferromagnetic materials, the relationship between the converter current and the magnitude of the

magnetic flux is complex. Before saturation, the two can be approximated as linear, with a higher slope. However, after the iron core is saturated, the relationship between the two becomes nonlinear, and small changes in magnetic flux can cause a sudden increase in current. Both excitation inrush current and sympathetic inrush current may generate large currents that can affect the system and protection. Considering the influence of iron core saturation characteristics, the waveform of the excitation inrush current and the parallel sympathetic inrush generated by AC side of the converter transformer is as follows:

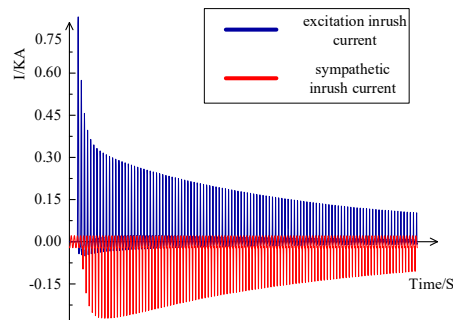


Fig. 2 Excitation surge, parallel sympathetic inrush waveforms

Observing the characteristics of the surge waveform in Fig. 3, it can be found that the excitation surge has the following features: larger amplitude, faster decay, after half a cycle to reach the maximum value, contains a large number of harmonic components of which the second harmonic is dominated by the waveform bias to the side of the time axis and the existence of intermittent angle. Corresponding to the parallel sympathetic inrush also has the following characteristics: the maximum value is less than the excitation inrush and the excitation inrush phase difference of  $180^\circ$  first increase and then decrease, slow attenuation of the core saturation direction and excitation inrush and the opposite. The inrush current phenomenon is characterized by significant harmonic components, with the second harmonic being particularly dominant. This harmonic content poses a serious risk of maloperation in differential protection schemes and other protective relays. Current harmonics of each frequency will induce voltage harmonics in the system, which directly cause the drop of AC bus voltage and affect the power quality. Distortion of voltage waveform can easily cause malfunction of broadband harmonic protection.

### 3. Study on the principle and action coefficient of broadband harmonic protection

#### 3.1 Wideband harmonic protection

Current harmonic components in the DC transmission system transfer process will cause impact on the equipment, in order to ensure good power quality and ensure the safe operation of the equipment, should be for the harmonic

generated by various ways to put forward the corresponding protection strategy. Broadband harmonic protection makes up for the shortcomings of harmonic distortion rate protection which only focuses on the integer harmonics and high harmonics and can detect and protect the voltage in a comprehensive way[15]. Fig. 4 presents the computational methodology for determining the operating coefficient in broadband harmonic protection systems.

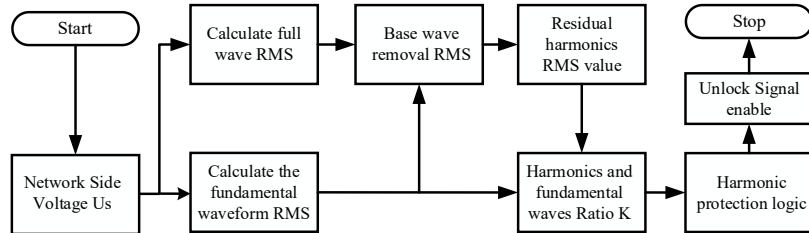


Fig. 4 Logic for calculating the operating coefficient of broadband harmonic protection

The execution of the protection action is mainly based on comparing the protection action coefficient  $K$  obtained by calculating the bus voltage with the preset protection setting value. This formula can be used to obtain the wideband protection action coefficient  $K$ :

$$k = \frac{U_{rms}^h}{U_{1rms}} = \frac{\sqrt{(U_{rms})^2 - (U_{1rms})^2}}{U_{1rms}} \tag{3}$$

This formula is come from the literature [15].In the formula,  $U_{rms}$  is the effective value of the full wave of the bus voltage,  $U_{1rms}$  is the effective value of the fundamental component of the bus voltage, and  $U_{rms}^h$  is the effective value of the harmonic component of the full voltage. In order to ensure the accuracy of the action of the broadband harmonic protection, it is necessary to add the second harmonic braking or other identification criteria for the inrush current of the converter transformer: if the inrush current of the converter transformer in the system is recognized, the protection will be blocked, and vice versa, the action will be taken when the voltage reaches the preset value and the broadband harmonic protection reaches the threshold of the action. The complete action logic of broadband harmonic protection is shown in Fig. 5.

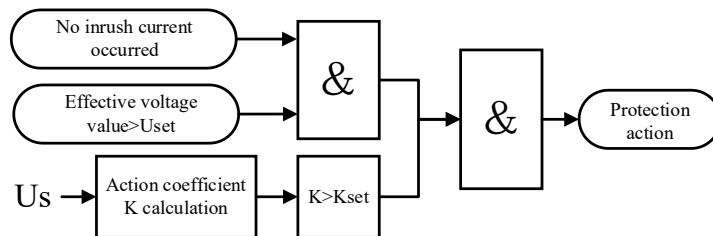


Fig. 5 Broadband harmonic protection action logic

That is to say, the action after the "&" symbol will only be triggered when all the conditions before "&" are met.

### 3.2 Analysis of the effect of converter transformer inrush current on broadband harmonic protection

The current harmonic content in the two inrush currents of transformers will be transmitted along the wire to the bus voltage, causing the voltage drop and distortion, resulting in the improvement of the protection action coefficient.

Analysis of the circuit shown in Fig. 2 shows that the common point voltage  $U_c$  has the following relationship with the bus current:

$$\vec{U}_c = U_s - I_s \times (R_s + jX_{Ls}) \quad (4)$$

Where  $R_s$  and  $X_{Ls}$  are the equivalent resistance and inductance on the voltage source and bus line respectively, and the bus current is related to the values of two types of inrush currents:

$$I_s = I_{t1} + I_{t2} \quad (5)$$

In this process, the voltage source inductor  $L_s$  exhibits different harmonic impedance in the face of each current harmonic:

$$X_{Ls} = 2\pi f \times L_s \quad (6)$$

It is not difficult to find that in the face of the same size of harmonic amplitude high-frequency harmonics in the power supply impedance will produce a greater voltage drop, making the bus voltage drop, elevated broadband protection action factor. The factors that may affect the size of the converter transformer inrush current will also affect the waveform of the bus voltage. Based on the simplified model derived from the transformer core flux formula and the above analysis, the following factors impact the inrush current magnitude: supply voltage, converter transformer impedance, power supply impedance, closing angle, residual flux, and system load conditions. Among these influencing factors, except for the closing angle and closing flux, they are all inherent parameters of the system that are difficult to change. Therefore, special attention should be paid to the effects of closing angle and remanence on the protective action coefficient.

In addition, load magnitude during the operation of the system directly affects the magnetic flux and current flowing through the running converter transformer. When the inrush occurs, the magnetic flux and inrush change on the basis of the original amplitude. Consequently, the size of the load connected to the converter is also one of the factors affecting the action coefficient of the broadband protection.

## 4. Calculation of dynamic broadband harmonic protection action thresholds

### 4.1 Study on the influencing factors of protection action coefficients

Three factors have the most significant influence on the protection action

factor during normal system operation: closing angle, residual flux, and load. The closing angle is mainly determined by the moment of closing, and is a random variable if the phase selection closing operation is not possible. Remanent magnetization is generated in a variety of scenarios, mainly caused by the breaking operation if the system is running normally, and there are many ways to measure other remanent magnetization scenarios. The load is determined by operational planning and is difficult to predict in advance.

Dynamic changes in the broadband harmonic protection action threshold should fully consider the three influencing factors, the different factors to take different ways of dealing with: to randomly determine the closing angle in accordance with the worst case of the impact of the influx of the value; residual magnetism is based on the last time the angle of tripping; the size of the load through the real-time monitoring of the system to be taken into account.

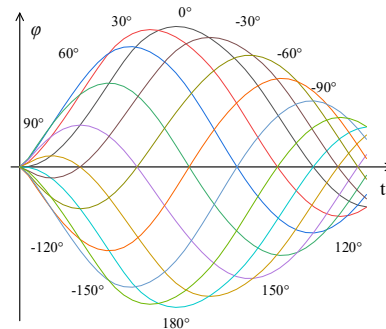


Fig. 6 The influence of closing angle on the magnetic flux of transformer core

Fig. 6 shows the relationship between the closing angle of the air dropped transformer and the change in magnetic flux of the iron core under the same residual magnetic field size. In the subsequent analysis, the influence of remanent magnetism and load conditions on the protection action coefficients should be analyzed according to the closing angle of  $0^\circ$ , so as to propose a dynamically varying protection action threshold.

#### 4.2 Working methods for dynamic protection action thresholds

The introduction of the dynamic protection action threshold for broadband harmonic protection is mainly to cope with the bus voltage distortion caused by the inrush current of the converter transformer, and it should mainly consider the working conditions that may generate inrush current and comprehensively consider all the influencing factors. In the normal operation of the system without the risk of inrush current of the converter transformer, it is necessary to reduce the action threshold.

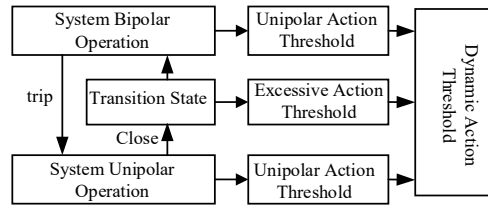


Fig. 7 Relationship between dynamic protection threshold and system operating status

Fig. 7 shows that the conversion between unipolar and bipolar operation is achieved by the tripping or closing operation of a branch. Dynamic protection action thresholds should have different action thresholds for different operation modes, which can be categorized into three types: the dynamic threshold for normal bipolar operation, the action threshold for unipolar operation, and the action threshold for the bipolar operation process from closing operation to system restoration of stability.

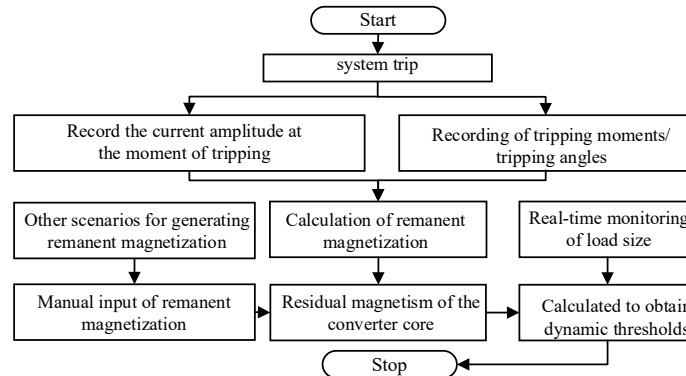


Fig. 8 Dynamic protection threshold calculation process

The inrush current of the converter transformer occurs in the transition state from unipolar operation to bipolar operation, during which the protection threshold should take into account both load and remanence factors. The load condition should be detected in real time, and the residual magnetization caused by tripping can be calculated based on the tripping angle and the current amplitude at the moment of tripping [16]. The residual magnetization caused by other conditions can be input manually. The expressions of remanence size, load and protection action threshold can be obtained by simulating and analyzing the parameters of the system in advance. The flow chart of calculating the real-time dynamic threshold that should be used in different application scenarios is shown in Fig. 8.

In order to reduce the possible impact of increasing the action threshold on the system, the calculated protective action threshold should be used immediately before the closing operation. After closing, the attenuation of the inrush is identified in combination with other criteria, and the normal protective action threshold can not be applied until the inrush is completely attenuated.

### 5. Simulation verification

This section takes the parameters of the converter transformer at Zhangbei DC Transmission Converter Station shown in Table 1 as an example, the total resistance of the selected power supply and the line in front of the transformer is 100 Ω, the traditional protection value is selected as 5% as the action threshold, the size of the second harmonic auxiliary criterion is selected as a fixed value of 43 A, and the transition state is set as the positive converter transformer is no-loaded and closed, and the negative converter transformer is normally operated before the closure. PSCAD software is used to build a simulation model to illustrate the calculation method of dynamic protection action threshold.

Table. 1

**Parameters of a certain converter transformer**

parameters	converter transformer
rated capacity	283.3MVA
transformation ratio	525/290.88
short circuit impedance	14.85%
No-load current	0.09%
Load Loss	501.69KW
leakage resistance	55132.6KW

The converter transformer station's unipolar normal operation is similar to the bipolar operation, Table 2 shows the changes in protection action coefficients of the two operation states are not much different in the occurrence of common faults:

Table. 2

**Comparison of K values during unipolar and bipolar operation faults**

Fault Type	Recording Moments	Unipolar operation (phase A/B/C) K%	Bipolar operation (phase A/B/C) K%
Single-phase ground fault	early stage of trouble	1.926/0/1.444	1.904/0/1.422
	Fault recovery	4.254/0.055/4.103	4.22/0.056/4.07
Two-phase ground fault	early stage of trouble	40.308/18.873/18.732	39.906/18.776/18.574
	Fault recovery	30.603/12.615/17.551	90.948/12.421/17.579
Three-phase ground fault	early stage of trouble	40.308/28.744/28.069	39.901/28.452/27.825
	Fault recovery	30.868/26.250/27.342	31.280/25.640/27.145

It also shows that the half-load situation is shown as an example respectively. The amplitude of protection action coefficients for unipolar and bipolar operation in the face of faults. The difference between the protected action coefficients for bipolar and unipolar operation under common fault types is not significant, so there is no need to set different action thresholds for the steady state of the two operation modes. According to the national standard, the voltage distortion rate should be less than 2%, and the conventional action threshold setting is generally set at 5%, which

is still used here for the steady state of unipolar and bipolar.

The key to the setting of the dynamic protection action threshold lies in the selection of the threshold for the transition process from unipolar to bipolar operation of the DC transmission system, where attention needs to be paid to the influence of two parameters, load and remanent magnetization, on the protection action coefficient. Normal operation of the transformer core internal flux is generally saturated flux of 0.6-0.8 times, may produce remanent magnetism is generally not more than 0.7 times the saturation flux, here respectively. DC transmission system in general is also difficult to inhibit the maintenance of full load operation; the impact of the load can be analyzed at 10% intervals to analyze the transmission system load from the rated capacity of 10%-120% of the range of analysis.

Considering the effect of load on the action coefficient of Converter Transformers in the Event of Surge Current alone, the magnitude of remanent magnetization can be regarded as a fixed value, and 0.4 times of the saturation flux can be taken here, and the relationship between the protection coefficient and the load can be found by changing the load condition. According to Fig. 9:

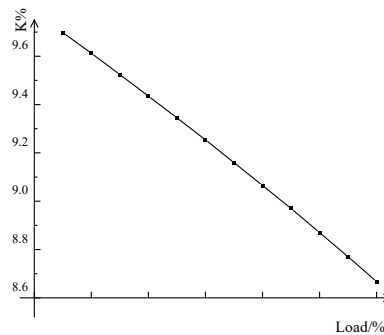


Fig. 9 The influence of load on the protection action coefficient

it can be seen that the relationship between the load and the protection coefficient of action is close to linear negative correlation, the larger the load the smaller the protection coefficient of action in the case of the same residual magnetization.

Considering the effect of remanence on the action coefficient of Converter Transformers in the Event of Surge Current alone can specify that the load value is constant, its size is half of the rated load, and the size of the remanence is 0-1 times the saturation flux for explanation. Fig. 10 shows that the relationship between the remanence and the protection action coefficient is obviously nonlinear, and it can be divided into two sections, which is similar to the conventional two-stage linear simplification of the hysteresis loop.

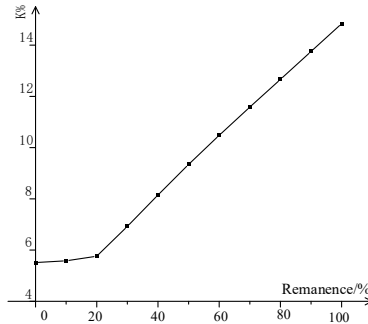


Fig. 10 The influence of residual magnetism on the protection action coefficient

The influence of the residual magnetism and the load size on the protection action coefficient during the transition state is considered, and the values are taken according to the variation of the load and the residual magnetism to obtain the possible protection action coefficient. The 132 data obtained were fitted to a two-dimensional polynomial nonlinear surface to obtain a formula with the remanence magnitude  $B_r$  and the load magnitude  $P$  as the independent variables and the protection action coefficient  $K$  as the dependent variable. Considering the possible errors in the fitting process and the margin between the protection threshold and the possible protection coefficients, the dynamic protection threshold that should be used in the transition process can be obtained by multiplying the whole equation by a factor of 1.2.

$$\begin{aligned}
 K_{set} = & 1.2 \times (6.03308 - 0.00379P + 1.24772 \times 10^{-5} P^2 \\
 & - 1.532 \times 10^{-8} P^3 - 1.17068 \times 10^{-10} P^4 \\
 & + 2.6435 \times 10^{-13} P^5 - 4.48865 B_r + 34.51635 B_r^2 \\
 & - 16.62417 B_r^3 - 19.5764 B_r^4 + 15.32452 B_r^5)
 \end{aligned} \quad (7)$$

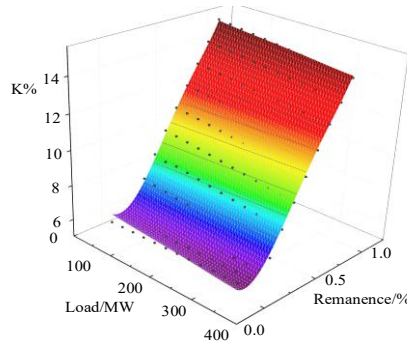


Fig. 11 Dynamic protection threshold fitting effect

Where  $K_{set}$  is the protection action threshold that should be preset before closing,  $P$  is in MW, and  $B_r$  is the percent value of saturation flux. Fig. 11 shows the relationship between the fitted formula and the original sampling points. According to the obtained remanent magnetization and load parameters, the real-time proper protection action threshold can be calculated based on this formula.

Table. 3

**Comparison of protection thresholds under special loads and residual magnetism conditions**

Br/%	Load/%	K%	Positive second harmonic	Negative second harmonic	Conventional Protection Action Threshold	Dynamic Protection Threshold
1.1	115	15.402	15.183	7.99	Bipolar misoperation	Bipolar correct action
1.1	15	16.197	143.5	90.75	Bipolar correct action	Bipolar correct action
0	115	5.616	9.16	0.217	Bipolar correct action	Bipolar correct action
0	15	5.45	34.29	0.0785	Bipolar correct action	Bipolar correct action
0.4	50	8.14	100.39	13.9	Positive correct blocking negative protection error	Bipolar correct action

Select extreme cases for large remanence with large load, large remanence with small load, small remanence with large load, and small remanence with small load, as well as the case where the system operates at half load and the remanence is half of the saturated remanence. Comparing the action differences between traditional protection thresholds and dynamic protection thresholds, the results obtained are shown in Table 3. From Table 3, it can be found that the use of dynamic protection thresholds can be correctly actuated at moments when the load is not small. The situation of a very small load in a DC transmission system is relatively rare; more common operating conditions are likely to be those between the first and last columns of the table. So compared to the traditional protection thresholds, the dynamic protection thresholds are more advantageous for the scenario in which the sympathetic inrush of the converter transformer triggers the wideband harmonic protection to malfunction. Considering the case of DC transmission system faults in the transition state, set the fault to occur 0.2s after closing the gate, and observe the protection action of the new protection action threshold value compared with the traditional static threshold value. The residual magnetization is selected as 0.4 of the saturation value, and the load is half-load, at which time the calculated dynamic protection threshold should be 9.74%.

Table. 4

**Comparison of fault protection threshold during surge current**

Fault Type	Ka%	Ka%	Ka%	Conventional Protection Action Threshold	Dynamic Protection Threshold
single-phase ground fault	2.158	1.802	1.779	Three-phase inactivity	Three-phase inactivity
two-phase ground fault	39.266	18.309	18.883	Three-phase equalization	Three-phase equalization
Three-phase ground fault	39.332	27.932	28.227	Three-phase equalization	Three-phase equalization

Short-circuit and ground faults between three-phase lines generate harmonics that have a small impact and a short duration. Therefore, in the occurrence of the smallest impact of single-phase short-circuit faults rely on the

traditional protection action thresholds cannot be fully dealt with, the engineering generally using a combination of various protection behaviors to deal with various types of faults. For the table 4 can be found: in response to the converter transformer inrush current occurs during the simultaneous occurrence of faults, the dynamic protection threshold and the traditional static protection threshold action state is consistent. In other words, the method of dynamically increasing the threshold for the transition process does not bring new disadvantages to the protection.

Combined with the verification of the above two aspects, it can be concluded that the dynamic protection action threshold can well cope with the malfunction of broadband harmonic protection during the inrush current generated by the converter closing, and compared with the traditional static protection action threshold, it does not add new problems. At the same time, the dynamic protection threshold also avoids the possibility of dealing with faults and leaks caused by blindly increasing the static action threshold.

## **6. Conclusions**

This paper investigates the complex inrush current phenomenon during converter transformers energization and its resulting broadband harmonic protection maloperation in HVDC transmission systems. The study analyzes factors affecting both the inrush current characteristics and the operating coefficient of broadband harmonic protection. Based on the distinct characteristics and effects of these three factors, we propose an optimized broadband harmonic protection method utilizing dynamic protection thresholds. Simulation results demonstrate the method's advantages: compared with traditional static protection thresholds, the proposed approach significantly reduces the probability of protection maloperation during transformer energization under normal operating conditions. Additionally, the protection threshold adjustment time is notably shorter without increasing the risk of protection failure. Consequently, this method enhances power system operational reliability.

However, this study still has certain limitations regarding the dynamic threshold analysis for both monopolar and bipolar stable operation modes in HVDC transmission systems. Future research could further investigate the impact of fault currents on protection schemes, propose dynamic thresholds specifically tailored for stable operating conditions, and thereby refine the functional scope of dynamic thresholds.

## **Acknowledgment**

This work is supported by the Science and Technology Project of State Grid Jibei Electric Power Co., Ltd. EHV Power Transmission Company. (Contract No. SGJBJX00JLJS2400786).

## REFERENCES

- [1] Mei J, Guo J, Diao W. "A Hybrid MMC Control Strategy to Enhance the Resilience of DC Transmission System," in *IEEE Transactions on Industrial Electronics*, vol. 71, no. 9, pp. 10930-10939, Sept. 2024,
- [2] Zhao Y, Crossley P. Impact of DC bias on differential protection of converter transformers. *International Journal of Electrical Power & Energy Systems*, 2020, 115(Feb.):105426.1-105426.10. DOI:10.1016/j.ijepes.2019.105426.
- [3] Mohan M, Vittal K P. Design and Simulation of Quadrilateral Relays in AC Transmission Lines with VSC-Based HVDC Systems under Phase-to-Ground Fault Condition. *U.P.B. Sci. Bull., Series C*, 2019, 81(3):153-168.
- [4] Heretik P, Kovac M, Smitkova M, et al. Analysis of Selected System Factors on Sympathetic Inrush Current of Shunt Wound Transformers. 2013.
- [5] Rudez U, Mihalic R. Sympathetic inrush current phenomenon with loaded transformers. *Electric Power Systems Research*, 2016, 138:3-10. DOI:10.1016/j.epsr.2015.12.011.
- [6] Richter M, Mehlmann G, Luther M. Impact of recovery and sympathetic inrush phenomena on VSC HVDC systems. 2022 57th International Universities Power Engineering Conference (UPEC), 2022:1-6.
- [7] Chen Y. Mechanism Analysis of Sympathetic Inrush in Traction Network Cascaded Transformers Based on Flux-Current Circuit Model. *Energies*, 2019, 12. DOI:10.3390/en12214210.
- [8] Emil Cazacu, Lucian Petrescu. Inrush Current Investigation for Single Phase Power Transformers by Means of Magnetic Material Core Characteristic. *U.P.B. Sci. Bull., Series C*, 2015 ,77(2):193-204.
- [9] Jin N, Xing J, Lin X. Countermeasure on Preventing Line Zero-Sequence Overcurrent Protection From Mal-Operation Due to Magnetizing Inrush. *IEEE Transactions on Power Delivery*, 2019, 35(3):1476-1487.
- [10] Qi X, Yin X, Zhang Z. Study on the Unusual Misoperation of Differential Protection During Transformer Energization and its Countermeasure. *IEEE Transactions on Power Delivery*, 2016.
- [11] Noshad B, Razaz M, Seifossadat S G. A Model for the Ultra-saturation Phenomenon During Energization of an Unloaded Power Transformer and Its Effect on Differential Protection. *Electric Power Components and Systems*, 2013, 41(9-12): 1129-1145. DOI:10.1080/15325008.2013.807895.
- [12] Vladislav Kuchanskyy, Olena Rubanenko. Influence Assessment of Autotransformer Remanent Flux on Resonance Overvoltage. *U.P.B. Sci. Bull., Series C*, 2020, 82(3):233-250.
- [13] Stipeti N, Filipovi-Gri B, Perkovic M. Impact of autotransformer inrush currents on differential protection operation. *Electric Power Systems Research*, 2023. DOI:10.1016/j.epsr.2023.109309.
- [14] Ali E, Malik O P, Abdelkader S et al. Experimental results of ratios-based transformer differential protection scheme. *International Transactions on Electrical Energy Systems*, 2019, 29(11). DOI:10.1002/2050-7038.12114
- [15] Jiang Chongxue, Ma Xiuda, Zou Qiang, et al. High frequency harmonic protection methods and engineering practices for flexible DC transmission systems *Power System Automation*, 2024, 48 (03): 150-158
- [16] Xing Yunmin, Luo Jian, Zhou Jianping, et al. Estimation of residual magnetism in transformer iron core *Power Grid Technology*, 2011, 35 (2): 4 DOI: CNKI:SUN:DWJS. 0. 2011-02-032.